Contents lists available at Science-Gate

International Journal of Advanced and Applied Sciences

Journal homepage: http://www.science-gate.com/IJAAS.html

Investigation steady state of DG systems according to power network of Iran

Seyed Morteza Moghimi [1,*], Abolfazl Elahimanesh [2]

[1]Department of Electrical Engineering, Jasb Branch, Islamic Azad University, Jasb, Iran
[2]Department of Electrical Engineering, University of Applied Science and Technology (UAST) of Qom, Qom, Iran

ARTICLE INFO

Article history:
Received 27 November 2015
Received in revised form
10 January 2016
Accepted 11 January 2016

Keywords:
34-Bus power network
Distributed generation units
The static load ability limit
Voltage stability
Voltage profile

ABSTRACT

In the paper, the impact of distributed generation (DG) on voltage stability and static load ability limit of the sample power grid in Iran has been studied. Therefore, by varying the amount and location of distributed generations in bus 34 standard test networks of Iran different generation models were made. Then, simulation by FORTRAN programming language was written on these models and the results of these simulations were analyzed. To determine the distributed generations' location for improvement the static load ability limit and voltage stability on the test network of 34 buses standard of Iran, The venin equivalent reactance was calculated and the weak buses of network was determined. As a result, it was shown that insert distributed generations on this buses in improving the static load ability limit voltage stability have a significant impact. Also, to see the increase in the load ability limit and voltage stability improvement, the different pattern was created. Then, the load ability and voltage stability was investigated.

1. Introduction

Penetration of distributed generation (DG) in power networks is increasing rapidly. This increase can be due to factors such as environmental concerns, power market restructuring and development of power generation technology in small volume (Atwa and El-Saadany, 2010). Along with increased use of renewable energy, developing the integration of distributed generations (Nikkhajoei, and Lasseter, 2009). Integration of distributed generations also face difficulties, which in the meantime, one of the most important aspects of voltage stability (Gomez et al., 2013; Eftekharnejad et al., 2013; Tonkoski et al., 2012). Stability analysis of the most important studies is in power grids. Instability and voltage collapse usually occurs on systems that are not capable of dealing with reactive power (Zhou et al., 2005; Moghimi et al., 2015).

Reactive power resources, network, network structure and generation pattern of active network buses voltage stability is an important factor affecting. Each of these factors can affect the way the system voltage stability margin of safety and a way for each defined critical status. Therefore, the main factor in determining the makeup of plant is generation system security feature. Penetration of DG on power systems, unlike the conventional mode of centralized generation model buses can be changed to be more flexible. This has an impact on the margin of voltage stability and voltage stability is security.

In the paper, aimed was assessed the effect of distributed generation on the voltage stability and the static load ability system. To determine the effects of the generation load and voltage stability of the system, network system 34 buses Iran test is used to study the steady state is selected. By analyzing the different modes and the results of similar models in this system, the effects mechanism of different generation systems on the behavior of the chargeability and voltage stability is analyzed. The rest of the paper is categorized. Section 2 34-bus test pattern generation networks and its impact on voltage stability are described. Section 3 describes the mathematical modeling problem. Section 4 simulation results stated. Finally, the conclusion expressed.

2. Bus test pattern generation networks in Iran and its effect on voltage stability

Extensive research programs in the second and third of Iran to prioritize the use of existing capacities in the field of renewable energy has been done. According to the program of development of Iran's Fourth Development Plan, in which the end of the program, one percent of the installed capacity of about 500 MW in the field of renewable energies be achieved. Authors have to use more and more

* Corresponding Author.
Email Address: Mortezamoghimi1990@yahoo.com (S.M. Moghimi)

economical feasibility of renewable energy and distributed generation power industry in Iran is under study. To investigate the effect of voltage stability and maximum loading patterns of generation on 34-bus test network is necessary to produce a variety of patterns created. Here, a number of different patterns of generation, as shown in Table 1 were prepared. It is possible to find a suitable model of generation, the network's 34-bus test to study the steady state is assumed. The system corresponds to the size and topology of the power system, to assess the changing pattern of generation and its impact on the load and voltage stability, has been appropriate. The test network is shown in Fig. 1 of 34 buses (Elahimanesh, 2004).

The system has a total of 34 buses and 73 line, is composed as follows: a slack bus (bus number 1), 13 generation buses (buses No. 3, 6, 8, 11, 12, 14, 19, 20, 21, 24, 27, 30, 32), consumption bus 20 (buses 2, 4, 5, 7, 9, 10, 13, 15, 16, 17, 18, 22, 23, 25, 26, 28, 29, 31, 33, 34). The results of the flow of the initial condition of the system show that the total system loads of 16524 MW. As well as, the loss is about 182 MW.

Table 1: Amount of coefficients (β) buses generation percentages in different patterns from 34-bus network

G.P. Bus	1	2	3	4	5	6	7	8	9	10	11	12	13	14
2	0.0	0.0	0.0	0.0	0.0	0.0	0.0	0.0	0.0	0.0	0.0	0.0	0.0	0.0
3	10.9	10.9	12.1	10.9	10.9	9.7	9.7	9.7	9.7	9.7	9.7	9.7	9.7	10.3
4	0.0	0.0	0.0	0.0	0.0	0.0	0.0	0.0	0.0	0.0	0.0	0.0	0.3	0.0
5	0.0	0.0	0.0	0.0	0.0	0.0	0.0	0.0	0.0	1.2	0.6	0.6	0.0	0.0
6	4.4	4.4	5.6	4.4	4.4	4.4	4.4	4.4	4.4	4.4	4.4	4.4	4.4	4.4
7	0.0	0.0	0.0	0.0	0.0	0.0	0.0	0.0	0.0	0.0	0.0	0.0	0.0	0.0
8	6.1	4.8	7.3	6.1	4.8	6.1	6.1	6.1	6.1	6.1	6.1	6.1	6.1	6.1
9	0.0	0.0	0.0	0.0	0.0	0.0	0.0	0.0	0.0	0.0	0.0	0.0	0.0	0.0
10	0.0	0.0	0.0	0.0	0.0	0.0	0.0	0.0	0.0	0.0	0.0	0.0	0.0	0.0
11	7.3	6.1	7.3	6.1	6.1	6.1	6.1	6.1	6.1	6.1	6.1	6.1	6.1	6.7
12	7.3	6.1	7.3	7.3	6.1	6.1	6.1	6.1	6.1	6.1	6.1	6.1	6.1	6.7
13	0.0	0.0	0.0	0.0	0.0	0.0	0.0	0.0	0.0	0.0	0.0	0.0	0.0	0.0
14	4.8	4.8	4.8	4.8	4.8	4.8	4.8	4.8	4.8	4.8	4.8	4.8	4.8	4.8
15	0.0	0.0	0.0	0.0	0.0	0.0	0.0	0.0	0.0	0.0	0.6	0.6	0.3	0.3
16	0.0	0.0	0.0	0.0	0.0	0.0	0.0	0.0	0.0	0.0	0.0	0.0	0.0	0.0
17	0.0	0.0	0.0	0.0	0.0	0.0	0.0	0.0	0.0	0.0	0.0	0.0	0.0	0.0
18	0.0	0.0	0.0	0.0	0.0	0.0	0.0	0.0	0.0	0.0	0.6	0.6	0.0	0.0
19	6.1	6.1	6.1	4.8	6.1	6.1	6.1	6.1	6.1	6.1	6.1	6.1	6.1	6.1
20	3.8	5.0	3.8	3.8	5.0	3.8	3.8	3.8	3.8	3.8	3.8	3.8	3.8	3.8
21	9.4	9.4	8.2	8.2	9.4	8.2	8.2	8.2	8.2	8.2	8.2	8.2	8.2	9.4
22	0.0	0.0	0.0	0.0	0.0	0.0	0.0	0.0	0.0	0.0	0.0	0.0	0.0	0.0
23	0.0	0.0	0.0	0.0	0.0	0.0	0.0	0.0	0.0	0.0	0.0	0.0	0.0	0.0
24	15.2	15.3	14.0	14.0	15.3	15.3	15.3	15.3	15.3	15.3	15.3	15.3	15.3	15.3
25	0.0	0.0	0.0	0.0	0.0	0.0	0.0	0.0	1.2	1.2	0.6	0.6	0.3	0.3
26	0.0	0.0	0.0	0.0	0.0	0.0	0.0	0.0	0.0	0.0	0.0	0.0	0.0	0.0
27	5.1	6.3	6.3	6.3	6.3	5.1	5.1	5.1	5.1	5.1	5.1	5.1	5.1	5.1
28	0.0	0.0	0.0	0.0	0.0	0.0	0.0	0.0	0.0	0.0	0.0	0.6	0.3	0.0
29	0.0	0.0	0.0	0.0	0.0	0.0	4.8	2.4	1.2	1.2	1.2	0.6	1.2	0.6
30	7.3	7.3	6.1	8.5	8.5	7.3	7.3	7.3	7.3	7.3	7.3	7.3	7.3	7.3
31	0.0	0.0	0.0	0.0	0.0	0.0	0.0	0.0	0.0	0.0	0.0	0.0	0.0	0.0
32	11.1	12.3	9.9	13.6	11.1	11.1	11.1	11.1	11.1	11.1	11.1	11.1	11.1	11.1
33	0.0	0.0	0.0	0.0	0.0	0.0	0.0	0.0	0.0	0.0	0.0	0.6	0.0	0.0
34	0.0	0.0	0.0	0.0	0.0	4.8	0.0	2.4	2.4	1.2	1.2	0.6	2.4	0.6

3. Mathematical modeling of problem

Bus voltage changes according to the load according to the P-V curve will be displayed. Points on the P-V curve is response of flow equations in different times. The first to achieve this curve must be added load parameter according to the following flow equations (Elahimanesh, 2004).

The packet flow equations, each bus i from a system n bus according to equation 1 is expressed.

$$\begin{cases} P(\delta, V, \lambda) = 0 \\ Q(\delta, V, \lambda) = 0 \\ 0 \le \lambda \le \lambda_{Max} \end{cases} \quad (1)$$

To solve the problem and finding the critical points, starting from a basic response and using the prediction / correction, the response is calculated at different load levels. The above process is as follows.

3.1. The step of new response prediction

Considering that close to the critical point flow equations are not well-behaved, so the process of prediction / correction is used. Predicting step for predicting the response to the increase in the new times (changing parameter of λ) from linear approximation equations was used. With the full differential flow equations, these equations have become a set of linear equations.

$$dP[(\delta, V, \lambda)] = P_\delta d\delta + P_V + P_\lambda = 0 \quad (2)$$
$$dQ[(\delta, V, \lambda)] = Q_\delta d\delta + Q_V + PQ_\lambda = 0 \quad (3)$$

$(Q_\delta)P_\delta$ Partial differential equation that the matrix contains active power (reactive) is based on the angle δ, $(Q_\delta)P_\delta$ the matrix of partial equations of active power (reactive) in terms of size and operating voltage of partial differential equations of active power (reactive) is based on parameters λ whose members are as follows:

$$P_\lambda^i = \frac{\delta P_i}{\delta \lambda} = P_{GiO}K_{Gi} - K_{PlLi}SC_{os\varphi_I} \quad (4)$$
$$Q_\lambda^i = \frac{\delta PQ_i}{\delta \lambda} = Q_{GiO}K_{Gi} - K_{PlLi}SS_{in\varphi_I} \quad (5)$$

Closed form of equations for equation 6 accordingly:

$$\begin{vmatrix}0\\0\end{vmatrix} = \begin{vmatrix}dP\\dQ\end{vmatrix} = \begin{vmatrix}P_\delta & P_V & P_\lambda\\ Q_\delta & Q_V & Q_\lambda\end{vmatrix}\begin{vmatrix}d_\delta\\d_v\\d_\lambda\end{vmatrix} \quad (6)$$

Matrix J is the conventional matrix of Newton-Raphson method. In equation 1 a variable λ flow equations has been added. Therefore, to solve with added equation is required. This can be used to identify the variables (variable continuous). (In the beginning step, variable of λ is selected as continuous variable). In other words, if the vector t used to represent vector variables the equation will be as follows:

$$t = [d_\delta \quad d_v \quad d_\lambda]^T, t_K = \pm 1 \quad (7)$$

Variable t_k as continuous variable is the positive and negative variable depending on the type and direction of the curve. By selecting one of the variables as continuous variables, equation 1 is soluble and made the following equations:

$$\begin{vmatrix}P_\delta & P_V & P_\lambda\\ Q_\delta & Q_V & Q_\lambda\\ & e_K & \end{vmatrix}\begin{vmatrix}d_\delta\\d_v\\d_\lambda\end{vmatrix} = \begin{vmatrix}0\\ \pm 1\end{vmatrix} \quad (8)$$
$$e_K = [0, \dots, 1, 0, \dots, 0] \quad (9)$$

All elements e_k except the k-th element is 1, equal to zero. Additional equation, e_k ensures that the Jacobian matrix equations is non-singular.

Select symbol of (+1) or (-1) as indicated on the form of the variables are continuous along. If the variable persistence over the course of increase, the (+1) and otherwise mark (1) is selected, and the selection of symbols corresponding element in the vector t is obtained. By solving the system of equations, the new points using the following equations are obtained:

$$\begin{vmatrix}d^*\\v^*\\\lambda^*\end{vmatrix} = \begin{vmatrix}\delta_0\\v_0\\\lambda_0\end{vmatrix} + \delta\begin{vmatrix}d_\delta\\d_v\\d_\lambda\end{vmatrix} \quad (10)$$

The parameter predicted values and σ to set the stride length is a scalar. The step shall select and adjust the response is expected within a radius of convergence.

3.2. The step of new response correction

After finding the answers; predicted which this action is necessary to calculate an exact answer is in the stage of correction. Power flow equations in correction step are as follows:

$$\begin{cases}P(\delta, V, \lambda) = 0\\ Q(\delta, V, \lambda) = 0\\ X_K = \eta\end{cases} \quad (11)$$

In the above equation, X_k variable duration and η variable continuity should be noted that the initial guess is equal:

$$\begin{vmatrix}\delta^*\\v^*\\\lambda^*\end{vmatrix}$$

The equations of Newton-Raphson method is as follows:

$$\begin{vmatrix}dP\\dQ\\0\end{vmatrix} = \begin{vmatrix}P_\delta & P_V & P_\lambda\\ Q_\delta & Q_V & Q_\lambda\\ 0, 0, \dots & 1, 0, \dots & 0\end{vmatrix} \quad (12)$$

Above equations are usual power flow equations. The difference is that a row and column has been added to it.

3.3. Choose continuity variable and understanding of the critical point

Selection of appropriate continuity correction is very important especially for the step, so a suitable choice for continuous parameter, the state variable is the biggest change. To remove columns on the bus has come to a critical state, with the state of the bus voltage variable change as a continuous parameter is selected.

$$X_K = |t_K| = max[|t_1|, |t_2|, \dots, |t_K|] \quad (13)$$

To identify the critical point, the tangential component of $\lambda(d\lambda)$ for the curve to the P-V, positive, and zero at the critical point in the lower curve is negative, so from the sign $d\lambda$ can be recognized above point.

3.4. Exceptional value theory

From exceptional value theory can be for determining the degree of voltage stability and voltage stability margin used buses. If the Jacobian matrix display, Hermitian this matrix is the following.

$$J^H = (J \times J^T) \quad (14)$$

While in equation 14, J^T is Transpose Jacobian matrix. The matrix specific amounts of the Jacobian

matrix multiplication in its Hermitian, some real and positive to the equation 15 are obtained:

$$det[I - \lambda j^H \times j] = 0 \quad (15)$$

Specific amounts of solving the above equation is showed with λ_K that some real and positive. Index K represents bus K-th of network. The square root of a value corresponding to Hermitian special, exceptional value that it has obtained the corresponding bus δ_K and have equal $\delta_K = \sqrt{\lambda_K}$ is presented.

3.5. Assess the voltage stability and security degree index

3.5.1. Voltage stability limit

Power flow equations Jacobian matrix Determinant can be used as a measure of distance or proximity to the border point of the system voltage stability, represents the margin of safety of the system. In point of voltage collapse, and consequently the amount of the standard system security margin will be zero.

The bus voltage changes amount to load changes $\frac{\partial V}{\partial Q}, \frac{\partial V}{\partial P}$ is the other criteria of voltage stability security degree. In point of voltage collapse, this amounts are large, so large amount can be used as a measure of distance or proximity to the border point is considered voltage stability.

3.5.2. Voltage stability margin

Voltage stability security margin is calculated as follows.

$$\delta_K = \sqrt{\lambda_K} \quad (16)$$

3.5.3. Determination of low voltage buses

Given that the curve (P-V) buses of the network, the slope of the tangent to the curve at the operating point, the weak buses, is higher than other buses. This means that with increasing load, the faster buses are close to the point of the knee of the curve and voltage collapse, if my bus, the slope of the curve (P-V) related to it shows with T_i, we have:

$$T_i = \frac{dV_i}{dP_{Total}} \cong \frac{\Delta V_i}{\Delta P_{Total}} \quad (17)$$

Therefore, P_{Total} the total active power load in the curve (P-V) buses, bus voltage variations, all of it has been measured.

$$max\left\{\left|\frac{\Delta V_1}{\Delta P_t}\right|, \left|\frac{\Delta V_2}{\Delta P_t}\right|, \dots, \left|\frac{\Delta V_3}{\Delta P_t}\right| \Longrightarrow weak\ bus \quad (18)$$

Because the value ΔP is the same for all buses, so the weakest bus, bus voltage have the most variation.

$$max\{|\Delta V_1|,\ |\Delta V_1|, \dots, |\Delta V_3|\} \Longrightarrow Weak\ bus \quad (19)$$

By reaching to voltage stability limit or point of collapse, value $\frac{dV^i}{dP}$ is equal infinite, and or in other words, $\frac{dP}{dV^i}$ is equal zero. Since it is easier to calculate $\frac{dP}{dV}$, this value more appropriate indicator for voltage stability of the system, which is defined as follows.

$$VSI = \frac{dP_{Total}}{dV_i} \quad (20)$$

Which V^i, the weakest bus voltage network is identified in the system. Because the value $\frac{dP}{dV}$ is negative, therefore the voltage stability index (VSI) is positive, the authors have defined it with a minus sign (Note that the curve (P-V), symbol dV, dP_T opposite each other).

3.6. Modeling constraints

3.6.1. V-Q Sensitivity analysis

In solution of power flow equations according to the Newton-Raphson, network constraints can be expressed linearly by the Jacobian matrix elements. Jacobian matrix elements, the sensitivity of the transition show bus voltage. V-Q sensitivity in a bus, V-Q curve slope at a given point displays. Positive values indicate the sensitivity of stable performance and the sensitivity is smaller, the system is more stable. Positive values indicate the sensitivity of stable performance and the sensitivity is smaller, the system is more stable. Conversely, a negative value, sensitivity, indicating a small negative performance is unstable and sensitive, showing the performance is very unstable. Because of the nonlinear nature of V-Q, sensitivity range of different conditions, a direct measure of the relative degree of stability has not been shown to express the (Elahimanesh, 2004).

3.6.2. V-Q Modal analysis

Voltage stability index calculation system can be reduced Jacobian matrix defined quantities and specific vector J_R (Elahimanesh, 2004) identified. V-Q is observed that the sensitivity of the individual modes can identify voltage collapse and instead, information about the combined effect of all modes provide reactive power and voltage changes.

3.6.3. The effect of DGs

3.6.3.1. The effect of DGs on voltage drop

The simple system RLC, it is assumed that P_L, Q_L once were active and reactive power and P_{DG}, Q_{DG} active and reactive power generated by the DG at the time, the line voltage without the presence of distributed generation, is:

$$\Delta V = E - V = I_{LD}(R + JX) \quad (21)$$

In the above equation, I_{LD} the load consumption current that equal with:

$$I_{LD} = \frac{(P_L - JQ_L)}{V} \quad (22)$$

As a result, then placement referred to in equation 21, in the presence of distributed generation, the above equation is expressed as follows:

$$\Delta V = \frac{RP_{DG} - P_L + X(Q_{DG} - Q_L)}{V} \quad (23)$$

This equation was observed up to a certain amount of active and reactive power produced by DG, line voltage drop can be reduced to a considerable extent, as this can help to share the voltage stability.

3.6.3.2. Calculate the buses Thevenin equivalent reactance

Since the Thevenin equivalent reactance value for each of the buses network X_{TH_i} can be strong and weak representation of its bus network. For this reason, a program was written to determine X_{TH} for buses. From equation 24, X_{TH} is obtained.

$$X_{TH_i}(k) = \frac{V(k) \times [V_0(k) - V(k)]}{Q_{inj}(1)} \quad (24)$$

Above steps with the amount of reactive power injection of six (three levels and three levels of negative and positive) was repeated and the average of six values have been calculated as X_{TH} bus K-th. In the case of generation buses calculation methods in a way that first-time player and addition to the bus voltage, the amount of reactive power generation has been recorded. Then, in the implementation of the power flow program to the second level, that bus as the bus has been introduced with the exception that the amount of reactive power of the buses that obtained in the previous step. In addition to injection reactive power, also is given to the bus; as with other steps of the calculation X_{TH} for load buses. Therefore, for all network buses (except Slack buses) X_{TH} corresponding to each of the buses is calculated.

4. The simulation results on the 34-bus test network

The paper's coding of simulation program is written FORTRAN programming language programming language is strong in the field of computing. The output of the program is to facilitate statistical analysis and evaluation of the results and graphs in Excel files placed. Each generation models needed to study at a separate sheet of Excel file is placed. The output includes output data obtained from the load at the point closest to the load consisting of active and reactive power generation and consumption, size and angle of buses and bus voltage at the point of load ability limit and collapse voltage is close to the limit. In addition, changes in system voltage stability index, intended to determine the weak buses in generation and an increase in load factor growth during system load, the output of this program.

In the paper, reactive power control range is about $-0.4P_n \leq Q_n \leq 0.6P_n$. P_n, Q_n Generation is active and reactive power bus desired respectively. In the simulation of the program, the initial values can be stored all the time. Also, the percentage share of the generation and consumption of each bus relative to the total load is determined at the beginning of the program. The initial increase in the rate of consumption of each bus and the resulting increase in the total load have also been specified. The plan was to load and operating point is determined. In terms of the analysis carried out on the results of the relationship between different patterns of generation and patterns of DG in particular, on the load and voltage stability, the more publicity, the 34-bus system of test network and analysis for simulating is selected. To compare the loading of each generation patterns to each other, Table 2 and Fig. 1 is presented. Also, to facilitate the survey of the impact of the change in the pattern of loading, generation and consumption data bus system for bar graph with different colors are displayed; with different colors together in Figs. 2 to 7 that correspond to the Tables 3 to 8 of the results of the power flow channel 34 buses given at the point of load ability for each generation patterns are displayed. The load ability and losses related to each of the patterns associated with each of the Figs stated.

Table 2: Load ability limit of 34-bus test network generation different patterns

G.P. No.	Limit Load (MW)	G.P. No.	Limit Load (MW)	G.P. No.	Limit Load (MW)
1	16669	10	26201	19	16671
2	16898	11	24517	20	23543
3	16904	12	24497	21	21461
4	16888	13	24724	22	23258
5	16890	14	27722	23	23921
6	24325	15	22204	24	27653
7	19351	16	17789	25	16671
8	24254	17	23586	26	22204
9	24094	18	18212	27	27234

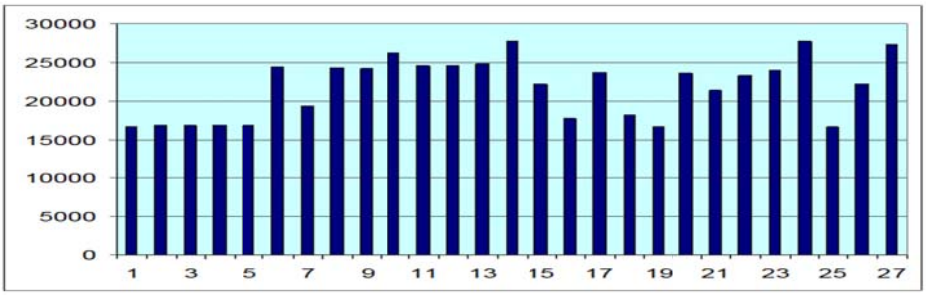

Fig. 1: Load ability limit of 34-bus test network generation different patterns

Table 3: Power flow results of 34–bus network at load ability limit point for the generation pattern No. 1

Bus No.	β (%)	P_G (MW)	Q_G (MVAR)	α(%)	P_L (MW)	Q_L (MVAR)	V (PU)	$\theta\|(DEG\|$
1	2.4	404	195	1.0	175	101	1.05	0
2	0.0	0	0	1.4	230	96	1	-2
3	10.9	1816	806	10.1	1691	811	1	-4
4	0.0	0	0	3.8	634	335	0.98	-8
5	0.0	0	0	2.3	377	114	0.97	-12
6	4.4	736	211	4.8	796	240	1	-13
7	0.0	0	0	2.2	364	162	0.99	-19
8	6.1	1009	168	0.2	40	7	1	2
9	0.0	0	0	3.0	502	58	1	1
10	0.0	0	0	3.6	608	223	0.98	-19
11	7.3	1211	228	5.4	905	417	1	-15
12	7.3	1211	207	5.3	883	277	1	1
13	0.0	0	0	0.6	98	43	1.01	2
14	4.8	807	68	2.2	368	87	1	2
15	0.0	0	0	1.2	202	71	0.93	-7
16	0.0	0	0	3.3	546	250	0.99	3
17	0.0	0	0	0.6	101	40	0.99	4
18	0.0	0	0	1.0	168	96	0.92	2
19	6.1	1009	113	2.7	453	178	1	18
20	3.8	626	157	2.8	469	195	1	10
21	9.4	1572	110	0.5	80	0	1	13
22	0.0	0	0	0.0	0	0	1	9
23	0.0	0	0	0.0	0	0	1	9
24	15.2	2542	1525	23.7	3953	1796	1	9
25	0.0	0	0	1.0	168	81	0.87	2
26	0.0	0	0	0.5	89	39	1	15
27	5.1	847	508	4.3	710	146	1	11
28	0.0	0	0	1.3	212	100	0.92	8
29	0.0	0	0	1.2	192	74	0.78	-2
30	7.3	1216	227	1.4	237	234	1	17
31	0.0	0	0	0.9	149	86	0.99	11
32	11.1	1856	285	4.1	689	205	1	17
33	0.0	0	0	1.7	286	156	0.95	13
34	0.0	0	0	1.8	296	169	0.62	-15
		P_G= 16860			P_L= 16669		P_{Loss}=191	
		Q_G= 4809			Q_L= 6886		Q_{Loss}= -2077	

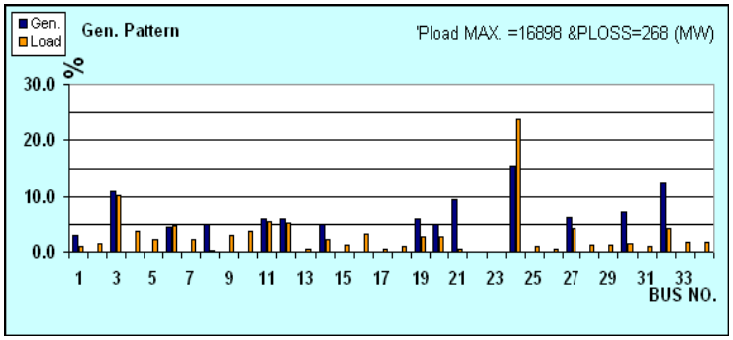

Fig. 2: Diagram of load and generation pattern No. 1 of 34–bus network and corresponding load ability limit

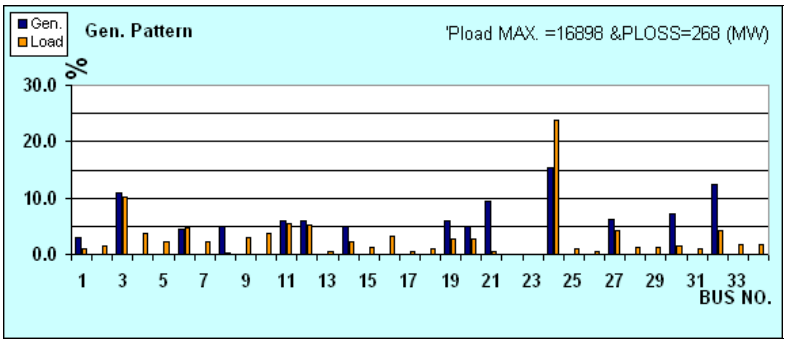

Fig. 3: Diagram of load and generation pattern No. 2 of 34–bus network and corresponding load ability limit

Table 4: Power flow results of 34–bus network at load ability limit point for the generation pattern No. 2

Bus No.	β (%)	P_G (MW)	Q_G (MVAR)	α(%)	P_L (MW)	Q_L (MVAR)	V (PU)	$\theta\|(DEG\|$
1	2.9	483	205	1.0	177	102	1.05	0
2	0.0	0	0	1.4	233	97	0.99	-2
3	10.9	1841	881	10.1	1714	822	1	-7
4	0.0	0	0	3.8	642	340	0.98	-11
5	0.0	0	0	2.3	383	116	0.96	-15
6	4.4	747	284	4.8	807	243	1	-20
7	0.0	0	0	2.2	369	165	0.98	-28
8	4.8	818	341	0.2	41	7	1	-1
9	0.0	0	0	3.0	509	58	1	-4
10	0.0	0	0	3.7	617	226	0.98	-31
11	6.1	1023	269	5.4	917	422	1	-29
12	6.1	1023	266	5.3	895	281	1	-4
13	0.0	0	0	0.6	99	44	1	-1
14	4.8	818	117	2.2	373	88	1	-3
15	0.0	0	0	1.2	205	72	0.92	-8
16	0.0	0	0	3.3	553	254	0.99	1
17	0.0	0	0	0.6	102	41	0.99	3
18	0.0	0	0	1.0	171	97	0.92	1
19	6.1	1023	123	2.7	459	180	1	20
20	5.0	839	175	2.8	476	197	1	17
21	9.4	1593	221	0.5	81	0	1	14
22	0.0	0	0	0.0	0	0	1	9
23	0.0	0	0	0.0	0	0	1	10
24	15.3	2577	1546	23.7	4007	1820	0.99	10
25	0.0	0	0	1.0	171	82	0.86	3
26	0.0	0	0	0.5	90	40	1	18
27	6.3	1064	541	4.3	720	148	1	17
28	0.0	0	0	1.3	215	101	0.92	11
29	0.0	0	0	1.1	194	75	0.76	1
30	7.3	1232	223	1.4	240	237	1	19
31	0.0	0	0	0.9	151	87	0.98	12
32	12.3	2086	321	4.1	699	208	1	20
33	0.0	0	0	1.7	289	159	0.95	16
34	0.0	0	0	1.8	300	172	0.58	-13
		P_G= 17166			P_L = 16898		P_{Loss} = 268	
		Q_G = 5514			Q_L = 6980		Q_{Loss} = -1467	

Table 5: Power flow results of 34–bus network at load ability limit point for the generation pattern No. 3

Bus No.	β (%)	P_G (MW)	Q_G (MVAR)	α(%)	P_L (MW)	Q_L (MVAR)	V (PU)	$\theta\|(DEG\|$
1	2.3	381	200	1.0	177	102	1.05	0
2	0.0	0	0	1.4	233	97	1	-2
3	12.1	2046	770	10.1	1715	823	1	-3
4	0.0	0	0	3.8	643	340	0.98	-7
5	0.0	0	0	2.3	383	116	0.97	-11
6	5.6	952	178	4.8	807	244	1	-10
7	0.0	0	0	2.2	369	165	0.99	-17
8	7.3	1228	2	0.2	41	7	1	2
9	0.0	0	0	3.0	510	58	1	-1
10	0.0	0	0	3.7	617	226	0.99	-18

11	7.3	1228	230	5.4	918	423	1	-13
12	7.3	1228	208	5.3	895	281	1	-1
13	0.0	0	0	0.6	99	44	1	0
14	4.8	819	71	2.2	373	88	1	0
15	0.0	0	0	1.2	205	72	0.92	-9
16	0.0	0	0	3.3	554	254	0.98	1
17	0.0	0	0	0.6	102	41	0.99	-1
18	0.0	0	0	1.0	171	97	0.91	-3
19	6.1	1023	129	2.7	459	180	1	15
20	3.8	634	155	2.8	476	197	1	9
21	8.2	1389	206	0.5	81	0	1	5
22	0.0	0	0	0.0	0	0	1	2
23	0.0	0	0	0.0	0	0	1	2
24	14.0	2374	1424	23.7	4009	1821	0.99	2
25	0.0	0	0	1.0	171	82	0.86	-6
26	0.0	0	0	0.5	90	40	1	9
27	6.3	1064	543	4.3	720	148	1	9
28	0.0	0	0	1.3	215	101	0.92	1
29	0.0	0	0	1.1	194	75	0.76	-9
30	6.1	1028	280	1.4	240	237	1	9
31	0.0	0	0	0.9	151	87	0.98	3
32	9.9	1678	311	4.1	699	208	1	8
33	0.0	0	0	1.7	290	159	0.95	4
34	0.0	0	0	1.8	300	172	0.58	-22
		P_G=17069			P_L=16904		P_{LOSS}=165	
		Q_G=4708			Q_L=6983		Q_{LOSS}=-2275	

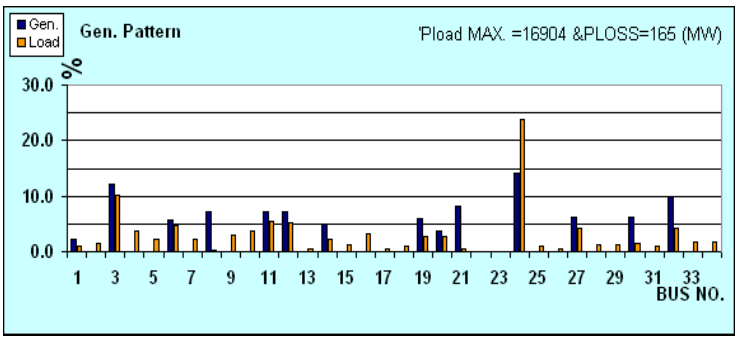

Fig. 4: Diagram of load and generation pattern No. 3 of 34–bus network and corresponding load ability limit

Table 6: Power flow results of 34–bus network at load ability limit point for the generation pattern No. 4

Bus No.	β (%)	P_G (MW)	Q_G (MVAR)	α(%)	P_L (MW)	Q_L (MVAR)	V (PU)	$\theta\|(DEG\|$
1	2.8	469	189	1.0	177	102	1.05	0
2	0.0	0	0	1.4	233	97	1	-3
3	10.9	1840	855	10.1	1713	822	1	-5
4	0.0	0	0	3.8	642	339	0.98	-9
5	0.0	0	0	2.3	382	116	0.96	-13
6	4.4	746	285	4.8	806	243	1	-17
7	0.0	0	0	2.2	369	165	0.98	-25
8	6.1	1022	247	0.2	41	7	1	2
9	0.0	0	0	3.0	509	58	1	-1
10	0.0	0	0	3.6	616	226	0.98	-28
11	6.1	1022	270	5.4	917	422	1	-26
12	7.3	1227	233	5.3	894	281	1	0
13	0.0	0	0	0.6	99	44	1	2
14	4.8	818	129	2.2	373	88	1	0
15	0.0	0	0	1.2	204	72	0.92	-8
16	0.0	0	0	3.3	553	253	0.99	3
17	0.0	0	0	0.6	102	41	0.98	4
18	0.0	0	0	1.0	171	97	0.92	2
19	4.8	818	121	2.7	459	180	1	15
20	3.8	634	156	2.8	475	197	1	9
21	8.2	1388	398	0.5	81	0	1	14
22	0.0	0	0	0.0	0	0	0.99	10
23	0.0	0	0	0.0	0	0	0.99	11

24	14.0	2371	1423	23.7	4005	1819	0.99	11
25	0.0	0	0	1.0	171	82	0.86	5
26	0.0	0	0	0.5	90	40	1	19
27	6.3	1063	541	4.3	720	148	1	19
28	0.0	0	0	1.3	215	101	0.92	13
29	0.0	0	0	1.1	194	75	0.76	3
30	8.5	1436	188	1.4	240	237	1	22
31	0.0	0	0	0.9	151	87	0.98	14
32	13.6	2290	370	4.1	698	207	1	23
33	0.0	0	0	1.7	289	158	0.95	19
34	0.0	0	0	1.8	299	172	0.58	-11
		P_G=17141			P_L=16888		P_{LOSS}=253	
		Q_G=5404			Q_L=6976		Q_{LOSS}=-1572	

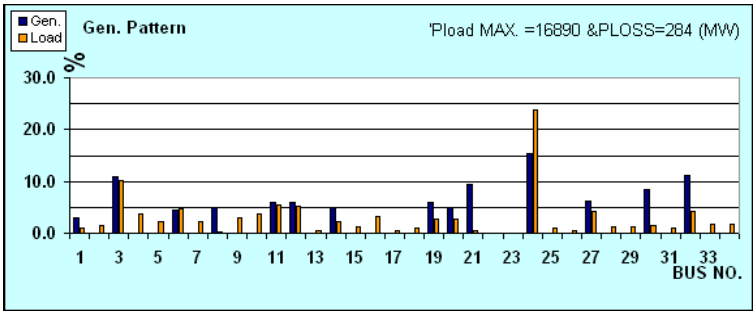

Fig. 6: Diagram of load and generation pattern No. 5 of 34–bus network and corresponding load ability limit

4.1. Analysis of different and patterns modes of Iran's 34-bus test network generation

In examining the results of different models of generation has been observed that some of the share transfer between buses produced by intensive generation, the amount of load ability and voltage stability, sensibly yet, but mortality has changed little. Put percent of generation is now concentrated in poor bus network voltage stability and maximum load ability has increased significantly. Also, the generation is now scattered on some poor bus network, increase voltage stability and maximum loading is to a large extent. The generation model No. 1 to 5, the percentage share of the generation of buses has been changed in various patterns. In this system, given the relatively low number of generation buses and the generation buses in different patterns, it is observed that the loading of each of these cases, the change is not significant, but their losses are significant changes there. In other generation models, from centralized to distributed generation of the load placed on the buses. It is observed that the DG on the bus load, generally to improve the load and voltage stability led. In particular, the weak buses now scattered time to put in place these buses, a significant improvement in the load and voltage stability of the system has created. Also, the generation model No. 6, some of the buses share of generation is reduced.

5. Conclusion

In this paper, improved voltage stability and the load ability limit on the test network 34-bus Iran to determine the steady state use of distributed generation were studied. By evaluating the results of the investigations carried out on the test network system 34-bus Iran, the effect of the distribution of the balance between load and generation on buses and put on weak buses of DG network to improve the load ability and voltage stability was viewed. Also, discussed the effects of DG time and reactive power control devices (such as svc) on voltage stability and determine the optimal location in power networks, the impact of dynamic voltage stability distributed generation with regard to limitation of reactive power and pulse changes transformers scattered by the authors for future research on the distributed generation and their impact on the power system is proposed.

References

Atwa YM and El-Saadany EF (2010). Optimal allocation of ESS in distribution systems with a high penetration of wind energy. Power Systems, IEEE Transactions on, 25(4): 1815-1822.

Eftekharnejad S, Vittal V, Heydt GT, Keel B and Loehr J (2013). Impact of increased penetration of photovoltaic generation on power systems. Power Systems, IEEE Transactions on, 28(2): 893-901.

Elahimanesh A (2004). Investigate distributed generations impact on stability voltage. M.sc. Thesis, Islamic Azad University, South Tehran branch, Tehran.

Gomez JC, Vaschetti J, Coyos C and Ibarlucea C (2013). Distributed generation: Impact on protections and power quality. Latin America Transactions, IEEE (Revista IEEE America Latina), 11(1): 460-465.

Moghimi SM, Amraii M, Salehi M, Zahedi AA and Shahnazi R (2015). Examine the role of voltage

stabilize and losses reduction effective approaches in the operation and design of distribution systems. Electronics Information and Planning, 3: 357-366.

Nikkhajoei H and Lasseter RH (2009). Distributed generation interface to the CERTS microgrid. Power Delivery, IEEE Transactions on, 24(3): 1598-1608.

Tonkoski R, Turcotte D and El-Fouly TH (2012). Impact of high PV penetration on voltage profiles in residential neighborhoods. Sustainable Energy, IEEE Transactions on, 3(3): 518-527.

Zhou F, Joos G and Abbey C (2005). Voltage stability in weak connection wind farms. In Power Engineering Society General Meeting. IEEE: 1483-1488.